Metallophysics and Advanced Technologies
Металофіз. новітні технол.
Metallofiz. Noveishie Tekhnol.
2024, vol. 46, No. 8, pp. 717–737
https://doi.org/10.15407/mfint.46.08.0717
Reprints available directly from the publisher

PACS numbers: 05.70.Np, 06.60.Wa, 68.08.Bc, 68.35.Np, 73.40.Jn

Abnormal Effect of Changing the Wetting Angle in Non-Equilibrium Melt–Solid Metal Systems

E. Ph. Shtapenko[*] and Yu. V. Syrovatko[*,**]

[*]*Ukrainian State University of Science and Technologies,*
2 Lazaryan Str.,
UA-49010 Dnipro, Ukraine
[**]*Dnipropetrovs'k Branch of the State Institution*
'Soils Protection Institute of Ukraine',
65[a] Naukova Str.,
UA-52071 Doslidne, Ukraine

The paper deals with the temperature dependence of the contact angle of wetting of a steel substrate with a liquid tin. The experiment shows that the wetting angle is decreased as the temperature rose, and the wettability of this system is improved. However, with the further increase in temperature, the contact angle is increased again that is an abnormal phenomenon. To explain this phenomenon and the process of contact-angle formation in general, we propose the quantum mechanical model based on the Wentzel–Kramers–Brillouin (WKB) conception. In this case, interaction of the melt ions with the substrate atoms is considered indirectly through the formation of a potential barrier with the linear dimensions determined by both the ratio of masses of the atoms of interacting metals and the temperature. From the WKB standpoint, at low temperatures, when the kinetic energy of a generalized particle with the reduced mass is less than the potential barrier, the wave function decays rapidly and, accordingly, the contact angle does not actually change. Quantitative and qualitative changes appear, when the kinetic energy of particles with the reduced mass exceeds the positive barrier values because of increase in temperature. Following the WKB conception, passage or reflection of a particle with the reduced mass over the barrier is determined by the integer or half-integer ratio of the de Broglie wavelength and linear dimensions of the potential barrier. Therefore, qualitative chang-

Corresponding author: Yuliya Volodymyrivna Syrovatko
E-mail: yu.syrovatko@gmail.com

Citation: E. Ph. Shtapenko and Yu. V. Syrovatko, Abnormal Effect of Changing the Wetting Angle in Non-Equilibrium Melt–Solid Metal Systems, *Metallofiz. Noveishie Tekhnol.*, **46**, No. 8: 717–737 (2024). DOI: 10.15407/mfint.46.08.0717

es in the system, *i.e.*, the wetting threshold and abnormal increase in the contact angle, are described by the processes associated with passage or reflection of a particle with the reduced mass over the barrier. Experimental and theoretical curves of dependences of both the contact angle and the work of adhesion *versus* temperature show similar dynamics.

Key words: temperature dependence of wetting angle, work of adhesion, passage of a particle over the potential barrier, reflection of the particle from the potential barrier, de Broglie wave, quantum number.

В роботі досліджено залежність крайового кута змочування рідким оливом підкладинки із криці від температури. У ході експерименту виявлено, що крайовий кут зменшується з підвищенням температури і поліпшується змочуваність даної системи. Однак з подальшим підвищенням температури крайовий кут знову збільшується, що є аномальним явищем. Для пояснення цього феномена, а також процесу формування крайового кута в цілому було запропоновано квантово-механічний модель, заснований на уявленнях Вентцеля–Крамерса–Бріллюена (ВКБ). У цьому випадку взаємодія йонів розтопу з атомами підкладинки розглядається опосередковано через формування потенціяльного бар'єра, лінійні розміри якого визначаються співвідношенням мас атомів взаємодійних металів і температурою. З позицій ВКБ за низьких температур, коли кінетична енергія усередненої частинки зі зведеною масою менша за величину потенціяльного бар'єра, відбувається швидке згасання хвильової функції і, відповідно, зміна крайового кута практично не відбувається. Кількісні та якісні зміни з'являються, коли кінетична енергія частинок зі зведеною масою перевищує значення позитивного бар'єра внаслідок підвищення температури. Відповідно до ВКБ-уявлень, проходження або відбивання частинки зі зведеною масою над бар'єром визначається цілим або напівцілим співвідношенням довжини де Бройлевої хвилі та лінійних розмірів потенціяльного бар'єра. Таким чином, якісні зміни в системі, такі як поріг змочування й аномальне збільшення крайового кута, описуються процесами, пов'язаними з проходженням або відбиванням частинки зі зведеною масою над бар'єром. Криві залежностей крайового кута та роботи адгезії від температури, побудовані експериментально та теоретично, мають подібну динаміку.

Ключові слова: температурна залежність кута змочування, робота адгезії, проходження частинки над потенціяльним бар'єром, відбивання частинки від потенціяльного бар'єра, де Бройлева хвиля, квантове число.

(Received 4 January 2024; in final version, 11 March 2024)

1. INTRODUCTION

Composite materials play an important role in the modern technologies. Composite materials with the metal matrix are used in various industries owing to their mechanical and tribological characteristics [1]. These materials are the result of the volumetric connection of two

or more materials based on adhesive bonds. As a rule, composites contain the materials with opposite properties (ductility and brittleness, stiffness and elasticity, conductors and dielectrics) [2–4].

In the manufacture of the composite materials, the processes of contact interaction at the filler–binder interface are to be strictly controlled. Implementation of these processes should ensure the required strength of the interfaces and, at the same time, it should not cause any unwanted phases to occur in the structure [5]. Therefore, in the processes of manufacture of the composite materials, attention is paid to determination of the value such as the work of adhesion between the structural components of composite materials and the nature of wetting of the filler with the molten binder [6–8]. The work of adhesion characterizes the interaction of two condensed phases per unit of contact area. The better the wetting of the solid phase with the liquid one and the smaller the wetting angle, the greater the work of adhesion [9].

The typical feature of systems where the chemical bonds between the liquid and the substrate material prevail is a strong dependence of the contact angles on temperature that is the wetting threshold is often present [10–13]. When the system is heated above the threshold temperature, the contact angle decreases because of significant rise in the work of adhesion.

To ensure better wetting during impregnation of the composite materials, soldering processes, *etc.*, it is necessary to determine the temperature at which the threshold for wetting of the solid phase with the liquid one occurs. Thus, calculation of the wetting threshold temperature holds the applied significance and is of interest from both practical and theoretical points of view.

The process of formation of the dynamic characteristics of liquid media, which determine the properties of surface phenomena and, consequently, the contact angle of a drop, is described in [14]. The paper uses the fundamental Euler and Navier–Stokes hydrodynamic equation and creates the original computerized modelling algorithm. This algorithm allows considering sufficiently large spectrum of statistical oscillations of the shapes and density of a drop of the liquid media, but generally, it cannot reflect the process of formation of the contact angle itself and, accordingly, the wettability properties in a fairly complete manner. Based on the computerized modelling of the modified Euler equations, the papers [15, 16] consider the Cahn–Hilliard equation taking into account the van der Waals interaction for isothermal liquids. Using the concept of the Ginsburg–Landau potential, this equation allows considering the formation of density distribution in the liquid drops and, in principle, to abandon the contact-angle indicator in the assessment of wetting properties [15].

Some other papers [17–20] also use the fundamental principles of computer model construction, including quantum mechanical con-

structs of multilayer structures forming the surface phenomena in the distribution of free energy and accordingly wetting properties.

The papers [21, 22] showed the increase of the contact angle in the systems with the temperature rise in the study of dependence of the contact angle on temperature. These cases of the contact-angle increase are considered abnormal ones. The authors of [21, 22] suggest that an increase in contact angles occurs owing to the formation of new chemical compounds between contacting substances or as a result of changes in the surface structure. In our opinion, this phenomenon is little studied and requires further research. Our paper presents the results of study of the temperature dependence of contact angle in the liquid tin–steel substrate system.

Wetting in liquid tin–steel substrate systems was previously studied in [23]. The paper [24] dealt with the dependence of contact angle in the liquid tin–iron substrate system. However, the phenomenon of abnormal increase of the angle was not found in Ref. [23, 24], since the temperature dependence of the contact angle was studied by continuous heating of the system to high temperatures. Consequently, no further increase in the angle with the temperature rise was observed in [23, 24] after decrease of the contract angle of wetting of the solid substrate with a drop of melt. In our experimental study, we supplied and examined a new individual drop of tin to construct each subsequent point of dependence of the contact angle versus temperature. Therefore, at each point of dependence, the contact angle was formed as new, that did not exclude its higher values compared to contact angles of previous drops of the substrate at the lower temperature. To explain this phenomenon and decrease in the contact angle at the wetting threshold temperature, this paper proposes the model representation based on the Wentzel–Kramers–Brillouin (WKB) semi-classical quantum conception.

2. EXPERIMENTAL TECHNIQUE

The contact angle of wetting of the steel substrate with liquid tin was determined by the sessile drop method [25]. For the experimental determination of the contact angle and the work of adhesion, tin alloys of the purity of 99.9995% wt. and steel of AISI 201 grade were used. Angles of wetting of the solid steel substrate with liquid tin were measured on the high-temperature unit with high stabilization of the temperature. To prevent the formation of unwanted compounds, heating was carried out in the nitrogen atmosphere, since no compounds are produced in the direct interaction of nitrogen and tin [26]. A drop of the substance under study was applied onto the substrate located on the object table of the working chamber through the bent fused silica capillary.

Figure 1 shows a drop of the substance after passing through the ca-

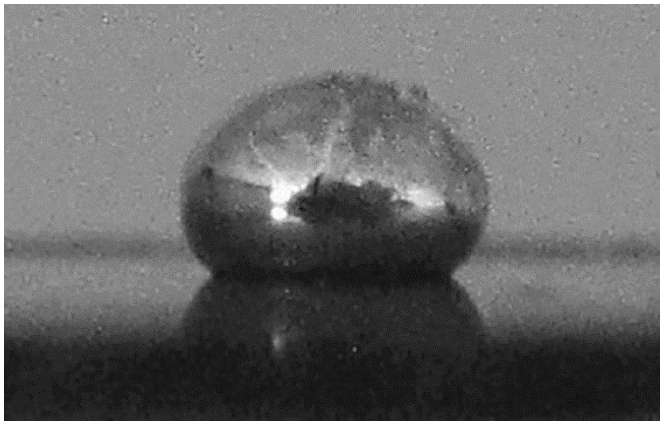

Fig. 1. A drop of liquid tin on a steel substrate of grade AISI 201.

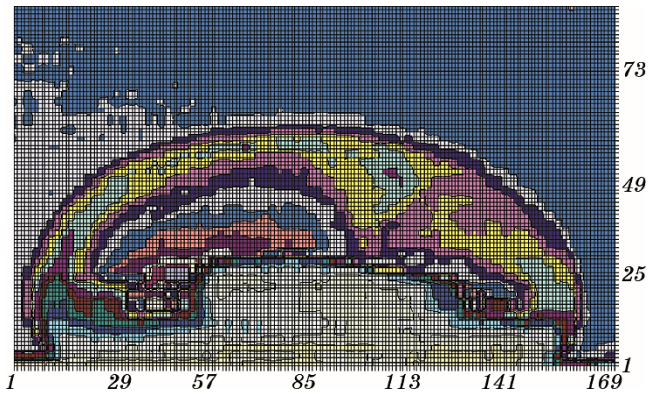

Fig. 2. Scanned image of a drop of liquid tin on a solid AISI 201-steel substrate.

pillary. The drop was held at the given temperature for 12 minutes. Then the furnace was cooled, the drop was removed, and the furnace was heated again to the higher temperature, and the next drop of liquid tin of the same type was fed through the capillary. Measurements were taken in the temperature range of 525–775 K with a step of 25 K. Contour of the drop was photographed using the digital camera. The resulting image was scanned and processed with the use of TLC-manager software [27]. When scanning the image, the program formed the matrices of light absorption coefficients corresponding to each pixel. Therefore, after scanning, a corresponding image was formed (Fig. 2) with the clear outline of the drop and the co-ordinate grid. After that, wetting angle of this drop was calculated. The work of adhesion of the corresponding system was calculated by the formula [28, 29]

$$A = \sigma(\cos\theta + 1), \tag{1}$$

where σ is surface tension of tin, θ is calculated contact angle of the system. To clarify the factors, which could affect the results of the experiment, studies of the chemical composition of the substrate and solidified tin drop using ion-selective [30] and atomic absorption [31] methods were carried out before and after the experiment. In addition, studies with the use of x-ray fluorescence method were conducted to detect iron atoms in a tin drop [32].

3. DEVELOPMENT OF THE THEORETICAL METHOD FOR DETERMINATION OF THE NATURE OF WETTING

3.1. Formation of the Potential Barrier in the Context of One-Dimensional Representation, Wave Packet and Interaction Conditions

When using this approximation, the description of interaction of the tin melt and iron substrate was built on quite simple principles of quasi-classical quantum mechanical concepts based on the WKB principles. We consider the direct interaction of a mobile tin atom and a stationary iron atom built into the crystal lattice of the substrate, *i.e.*, the specific laboratory system. During transition to the centre-of-mass system, an idea arises that a particle with the reduced mass m moves in a particular field (in our simplified case, it is one-dimensional field). Potential energy of this field is formed as a barrier owing to the interaction of similarly charged ions of the melt and the substrate. According to the known concepts, transmission coefficient shall be determined by the relation [33]

$$T(E) = (1 + ((k_2^2 - k_1^2) / 2k_1k_2)^2 \sin^2 k_2 l)^{-1}, \tag{2}$$

where $k_1 = \sqrt{2mE} / \hbar$, $k_2 = \sqrt{2m(E-U)} / \hbar$; $m = m_1m_2/(m_1 + m_2)$ is reduced mass, m_1 is melt atom mass, m_2 is substrate atom mass, $\hbar$ is Planck's constant, E is a total energy of the system, $E - U = K = k_BT/2$ is kinetic energy of the movement of melt and vibrations of the iron atom in the substrate, k_B is Boltzmann's constant, T is temperature, U is potential energy of the barrier, l is barrier width. Ultimately, particle with the reduced mass passes over the barrier under the conditions $\sin(k_2 l) = 0$, $(k_2)_n l = \pi n$, and

$$E = \frac{\pi^2\hbar^2}{2ml^2} n^2 + U, \; n = 1, 2, 3, \ldots. \tag{3}$$

Let us remark here that n has the meaning of a certain quantum number and satisfies the condition $l = (\lambda_n/2)n$, $\lambda = 2\pi/k_2$ is the

de Broglie wavelength. In this case, the integer number of half-waves is laid above the barrier. It is not necessary for n to have the large value in this expression; it may have small values.

In the event that $\sin(k_2 l) = \pm 1$, $l = (n + 1/2)\pi$,

$$E = \frac{\pi^2 \hbar^2}{2ml^2}(n + 1/2)^2 + U, \tag{4}$$

and total reflection should be observed. Given that $K = E - U$, kinetic energy of a particle with the reduced mass m, is determined by the temperature: it depends on $k_B T/2$ in the one-dimensional representation. In this case, even taking into account the statistical distribution of individual particles by speed and potential-energy formation, *i.e.*, barrier, with the temperature change, there should be a deviation from the monotonic dependence of the contact angle and, as a consequence, the change in the reflection coefficient. This dependence shall not have a sharp abrupt change, but it is quite measurable and may have the relatively pronounced amplitude range.

Further construction of the proposed model involves estimation of the potential barrier width. For this purpose, it is necessary to form quasi-classical representation of the wave function.

The process of contact of the melt with the surface can be represented in quasi-classical approximation as a total flow of non-interacting particles, where each of them can be described by its own wave function that can be compared with the wave packet. Its average value of the co-ordinate, *i.e.*, the total flow of particles, can be represented as

$$f(x) = \sum_k \sum_m a_m^* a_k f_{km} e^{i\omega_{km} t},$$

where $1 << k << \infty$, *i.e.*, the wave-packet condition is satisfied, f_{km} is matrix element, ω_{km} is transition frequency, x is co-ordinate, t is time, a_k, a_m^* are coefficients of expansion of the wave function $\psi = \sum_k a_k \psi_k$.

Coefficients a_k differ significantly from zero for the wave packet in the range of numbers of $1 << k << \infty$ and are close in value to each other. If we change the form of $s = k - m$, the previous equation can be rewritten as

$$f(x) = \sum_n \sum_s a_{s-k}^* a_k f_{km} e^{i\omega_s t}.$$

Since the coefficients a_{s-k} and a_k in the range of k numbering are close to each other, we can write

$$f(x) = \sum_n |a_k|^2 \sum_s f_s e^{i\omega_s t}, \sum_n |a_k|^2 \approx 1.$$

That is, matrix elements are transformed into the coefficients of the Fourier series. Generally, for each particle from the k spectrum, we can write

$$f_k = a_k^2 \sum_s f_s e^{i\omega_s t_k}.$$

Therefore, each particle can be separated from the others in its own time t_k. The wave function can be represented as the product of the number of elements of the wave packet and the wave function of an individual component.

3.2. Formation of Quasi-Classical Wave Function in the WKB Representation

Taking into account the time component, it is possible to form the wave function, the value of which decays exponentially inside the potential barrier when $|U| > |E|$. In this case, passage through the barrier significantly reduces the amplitude of the wave function, which generally corresponds to the absence of passage or reflection of the particle. Obviously, this condition is satisfied at low temperatures. For high temperatures in the order of the melt temperature, $|E| > |U|$. Here, we shall observe the passage at integer n and, accordingly, the reflection at half-integer $n + 1/2$. So, for the wave function, it is possible to write

$$\psi = \frac{NC}{2\sqrt{p_1}} \exp\left(\frac{i}{\hbar}\left|\int_a^b p(x)dx\right|\right) \exp(Kt_k / \hbar), \left|E\right| > \left|U\right|, \tag{5}$$

where N is number of components in a wave packet, C is coefficient, $p(x)$ is impulse of the particle, p_1 is impulse of a fast particle of the melt; a, b are boundaries of integration. This representation of the wave function is quite acceptable, since the coefficients determining the amplitudes in the wave packet do not differ much from each other. So, the wave function can be expressed as the product of the individual component by the number of components N. It should be noted that the values of p_1 and p in these expressions are not identical; it follows from the considerations below. Value of the impulse in the amplitude of the wave function is determined by the second term in the expansion with respect to the small parameter $\hbar$ of the quasi-classical function $\psi \sim \exp(i\mu / \hbar)$, where $\mu = \mu_0 + i\hbar\mu_1$, $\mu_0 \sim \pm\int p(x)dx$, $\mu_1 \sim \ln p^{1/2}$ [33]. When substituting into the function $\sim \exp(i\mu_1 / \hbar)$, the value of p_1 is in the denominator. It means that, with the increase in speed, a particle in the given volume is less likely to be detected. Therefore, the value of p_1 is determined by fast particles, *i.e.*, melt ions in the laboratory co-

ordinate system. Impulse of a fast particle of the melt can be correlated with the de Broglie wave of the given particle. From these considerations, we can also assume that, in the centre of mass system, the radius vector of fast particle of the melt is of the order of the de Broglie wavelength. Then, we can write:

$$p_1 = \frac{\hbar}{r} = \frac{\hbar m_2}{(m_1 + m_2) r_1} = \frac{m_2 \sqrt{2m_1(E-U)}}{(m_1 + m_2)}, \; r_1 = \frac{\hbar}{\sqrt{2m_1(E-U)}}, \; m_1 < m_2, \quad (6)$$

$$p_1 = \frac{\hbar}{r} = \frac{\hbar m_1}{(m_1 + m_2) r_1} = \frac{m_1 \sqrt{2m_2(E-U)}}{(m_1 + m_2)}, \; r_1 = \frac{\hbar}{\sqrt{2m_2(E-U)}}, \; m_2 < m_1, \quad (7)$$

where r is radius vector of a particle with the reduced mass in the field of potential energy U.

3.3. Normalization of the Wave Function and Calculation of the Barrier Width

The coefficient C in Eq. (5) is found from the Bohr–Sommerfeld quantization rule [33]. The wave function at the point $x = b$ results in the wave function

$$\psi = \frac{C}{\sqrt{p_1}} \cos\left(\frac{1}{\hbar} \int_b^x p dx - \frac{\pi}{4} \right). \quad (8)$$

During normalization of the wave function, it is sufficient to integrate $|\psi|^2$ only in the interval of $b \le x \le a$, since, beyond this interval, the function $\psi(x)$ has small values, because the coefficients of expansion of the wave packet are actually equal to zero. The square of sine can be replaced by its average value, *i.e.*, $1/2$. Then, we get

$$\int |\psi|^2 dx \approx \frac{C^2}{2} \int_b^a \frac{dx}{p(x)} = \frac{\pi C^2}{2m\omega} = 1, \quad (9)$$

where $\omega = 2\pi/t$ is frequency of the classical periodic motion. Consequently,

$$C = \sqrt{4m / t}. \quad (10)$$

The wave function taking into account the time component has the form:

$$\psi = \frac{NC}{2\sqrt{p_1}} \exp\left(\frac{i}{\hbar} px \right) \exp\left(\frac{Kt_n}{\hbar} \right). \quad (11)$$

Using the normalization condition for the co-ordinate component, we can write

$$D^2 \int_{-\infty}^{\infty} \exp(i(p - p')x / \hbar) dx = 1 . \tag{12}$$

All components associated with the co-ordinate component, including time-dependent components, are considered as D^2.

Further, from (12), we shall write

$$D^2 \int_{-\infty}^{\infty} dx \int_{-L}^{L} \frac{\exp(i\alpha x)}{x} d(\alpha x) = 1 , \tag{13}$$

where $\alpha = (p - p') / \hbar$. The inner integral is written and integrated as follows:

$$\begin{aligned} \frac{1}{x} \int_{-L}^{L} \exp\left(i\alpha x\right) d(\alpha x) &= \frac{1}{x} \int_{-L}^{L} \cos(\alpha x) d(\alpha x) = \\ &= \frac{1}{x} \sin(\alpha x)\Big|_{-L}^{L} = \frac{\sin(Lx) - \sin(-Lx)}{x} . \end{aligned} \tag{14}$$

Since $\sin(Lx)$ is the uneven function, we get from Eq. (14):

$$\frac{1}{x} \int_{-L}^{L} \exp\left(i\alpha x\right) d(\alpha x) = \frac{2}{x} \sin(Lx) . \tag{15}$$

If we represent p' as $-p$, *i.e.*, impulse, which is opposite by direction, but equal in value, that is the extreme value in the continuous spectrum of integration from $-L$ to L, we can determine the value $L = 2p / \hbar$, and the following expression is written

$$\int_{-\infty}^{\infty} \psi_p^* \psi_{p'} dx = 2 \int_{-\infty}^{\infty} \frac{\sin\left(\frac{2p}{\hbar} x\right)}{x} dx . \tag{16}$$

Considering the rapid convergence of the integral (16), we can replace the boundaries of integration by co-ordinates determining the extent of the energy barrier $\propto$ (0—l); then, from (16) we write:

$$2D^2 \int_{0}^{l} \frac{\sin\left(\frac{2px}{\hbar}\right)}{\frac{2px}{\hbar}} d\left(\frac{2px}{\hbar}\right) = 2D^2 \int_{0}^{l} \frac{\sin\beta}{\beta} d\beta = 1 , \tag{17}$$

where $\beta = 2px / \hbar$. Since the value $\overline{\beta} = 1$, by neglecting unity after integration, we obtain from (17)

$$\cos\left(\frac{2pl}{\hbar}\right) = \mathrm{Re}\left[\exp\left(-i\frac{2pl}{\hbar}\right)\right]. \tag{18}$$

After estimation of the co-ordinate component and return to the original expression for normalization of the wave function, considering the time component, we write

$$-\frac{NC^2\hbar}{8p_1 2p}\exp\left(-i\frac{2pl}{\hbar}\right)\exp\left(\frac{2Kt_k}{\hbar}\right) = 1, \tag{19}$$

where $C = \sqrt{4m/t}$.

Performing one-term expansion of the time component, we express the dimensions of the potential barrier. In the statistical aspect, when we consider separation of each particle in the wave packet in time, the total time of interaction with the substrate can be represented as $\tau \approx Nt_k$. Then, we can write

$$l = \frac{\hbar}{2p}\ln\left(\frac{K\tau m}{tp_1 p}\right), \tag{20}$$

where τ is time of contact of interacting phases, t is period of quasi-classical motion of the particle.

Dimensions of the potential barrier and, accordingly, the number n are determined by the set of components (p, p_1, m, K, τ, t) establishing a certain connection between l and n. Further, using the Bohr–Sommerfeld quantization expression [33]

$$\frac{1}{\hbar}\int_0^l \sqrt{2mK}\,dx = \pi n - \pi/2, \tag{21}$$

where the upper limit of integration is determined by linear dimensions of the potential barrier, we determine the number n. In this approximation, taking into account possible deviations from integer values in the calculations, the number n is actually the same with the value ≈ 6.

3.4. Non-Wetting, Wetting and Abnormal Increase in the Contact Angle

Now we shall consider the system at the initial temperature of 525 K (slightly above the melting point of tin). Here, we observe non-wetting of the liquid phase with the solid phase and assume that the particle passes over the barrier. In this case, the condition (3) is to be satisfied, *i.e.*, kinetic energy of the particle with the reduced mass will be

$$(E-U)_n = \frac{\pi^2\hbar^2 n^2}{2ml^2},\ n = 6. \tag{22}$$

For wetting to be observed in the system, the particle should be reflected from the barrier, *i.e.*, kinetic energy of the particle from Eq. (4) should be equal to

$$(E-U)_{n+1/2}=\frac{\pi^2\hbar^2(n+1/2)^2}{2ml^2}. \tag{23}$$

Then, we find the difference of energies (23) and (22), *i.e.*, the energy under which the system quantum number will change from the integer to half-integer, and the particle is reflected from the potential barrier:

$$\Delta(E-U)=\frac{\pi^2\hbar^2}{2ml^2}(n+1/4). \tag{24}$$

The system is capable of obtaining this energy when the temperature increases. Consequently, energy of the system $K_n=k_BT_n/2$, comparable to $(E-U)$ at the initial temperature, should increase by the value (24). Then, the final value of this quantity is

$$K_{n+1/2}=K_n+\frac{\pi^2\hbar^2}{2ml^2}(n+1/4)=\frac{1}{2}k_BT_{n+1/2}. \tag{25}$$

From Eq. (25), we find the temperature $T_{n+1/2}$, at which the particle reflection from the barrier and wetting of the solid phase with the liquid phase in the system is observed. At this temperature, a sharp decrease in the contact angle shall be observed.

Now, we shall determine the distance between adjacent energy levels, *i.e.*, the energy required for the quantum number of the system to change by unity and for the particle to pass through the potential barrier again. Kinetic energy of the particle located at energy level $n+1$ is

$$(E-U)_{n+1}=\frac{\pi^2\hbar^2(n+1)^2}{2ml^2}. \tag{26}$$

Difference of energies (26) and (22) is, accordingly,

$$\Delta(E-U)=\frac{\pi^2\hbar^2}{2ml^2}(2n+1). \tag{27}$$

Transition of the particle to the next energy level can be accompanied by deterioration of the wetting and increase in the contact angle. In the same way, we add (27) to the initial kinetic energy K_n at the initial temperature and find the temperature T_{n+1}, at which we observe the deteriorated wetting:

$$K_{n+1}=K_n+\frac{\pi^2\hbar^2}{2ml^2}(2n+1)=\frac{1}{2}k_BT_{n+1}. \tag{28}$$

Analysing the expressions (20), (24) and (27), we can come to the conclusion that increase in the quantum number in the relation (24) leads to the temperature rise in the system indirectly through kinetic energy and, accordingly, through the impulse by a certain value. At the same time, according to Eq. (20), impulse is directly involved in the calculations of the potential barrier, and its increase will lead to narrowing of the barrier in accordance with the temperature rise, adequate to the increase in energy when the quantum number becomes higher. Taking into account this relationship, in our opinion, it is logical to adopt the fixed dimension of the barrier in Eqs. (24) and (27), corresponding to the initial temperature close to the melting point of melt. Therefore, modelling of the dynamics of temperature rise is possible by increasing the quantum number in Eqs. (24), (27) and, respectively, comparing the theoretical dynamics of the contact angle temperature dependence to the experimental one.

4. THEORETICAL METHOD FOR CALCULATION OF THE WORK OF ADHESION

In this model representation, it is possible to consider the issue of the work of adhesion, linking it with the wetting phenomenon. That is, non-wetting is observed during passage of the barrier, while wetting is seen during reflection from the barrier. In accordance with the model representations, the passage amplitude takes the form [33]

$$t = \frac{4k_1k_2}{(k_1 + k_2)^2 - (k_1 - k_2)^2} \exp(i2k_2\gamma) .$$

Accordingly, the transmission coefficient is

$$T(E) = t^2 = \left[1 + \left(\frac{(k_2^2 - k_1^2)}{2k_1k_2} \right)^2 \sin^2(k_2\gamma) \right]^{-1} ,$$

where γ is certain phase determined by the barrier dimension l. If $\sin(k_2\gamma) = 0$, $(k_2 n)l = \pi n$, $T(E) = 1$, passage occurs over the barrier with no wetting. In this case, the work of adhesion can be expressed as

$$A = \frac{U}{2\pi\lambda^2} . \tag{29}$$

This expression is formed based on the representation of the barrier dimension normalization in the de Broglie wavelength units and dimensional requirements. Next, we shall find the height of the potential barrier.

From Ref. [33], it follows that

$$T = \frac{4E(E-U)}{(2E-U)^2} = 1. \tag{30}$$

The potential energy is represented as

$$U = -((E-U) + (U-K)). \tag{31}$$

After expressing $(E-U)$ from Eq. (30) and substituting in Eq. (31), we obtain

$$-2U = \frac{(2E-U)^2}{4E} - K = \frac{((E-U)+E)^2}{4E} - K. \tag{32}$$

To describe fully the solution, there are no sufficient input variables in the relation (32); so, in this case, we used the combined variable $(E-U)$ as a parameter. We obtained a family of solutions depending on the ratio of variables included in the combined parameter. Further, after analysis of the family of solutions, we chose the solution, which was the most appropriate for the description of real dependences obtained from experiments that is the contact angle as a function of time and temperature. Components included in the optimal parameter, which determined the optimal solution, were chosen with the use of computer modelling.

Therefore, the expression for U depending on $(E-U)$ and K in the case, when the particle passes over the barrier, is obtained as follows:

$$U_1 = \frac{-6K - 2(E-U)}{18} + \\ + \frac{1}{18}((6K + 2(E-U))^2 - 36(-3K^2 + (E-U)^2 + 2K(E-U)))^{1/2}. \tag{33}$$

In case of reflection, which can be achieved with a minimum transmission coefficient, *i.e.*, $\sin(k_2\gamma) = \pm 1$, $(k_2 n)l = (n + 1/2)\pi$, wetting is observed.

Then, the reflection coefficient is

$$R = 1 - T = \left(\frac{U}{2E-U}\right)^2 = 1. \tag{34}$$

From here,

$$4(E-U)E - U^2 = -U^2. \tag{35}$$

Using Eq. (31), we get

$$4(E-U)E - U^2 = -((E-U) + (U-K))^2. \tag{36}$$

Solving in the same way, we find the expression for the height of the potential barrier from Eq. (36) for the case of the particle reflection from the barrier

$$U_2 = \left| \frac{-2K(E-U) - (E-U)^2 - K^2}{6(E-U) - 2K} \right|. \tag{37}$$

Substituting U_1 or U_2 in the expression (29), we find the work of adhesion for the case of non-wetting (U_1) or for the case of wetting (U_2). The parameter $(E-U)$ is, respectively, expression (22) at a given temperature.

Contact angle of wetting of the solid phase with the liquid one is calculated by formula [29]

$$\theta = \arccos(A / \sigma - 1). \tag{38}$$

In conclusion, it should be noted that it is quite acceptable to use the quasi-classical approximations within the WKB representation, since the condition below is satisfied [33]:

$$\frac{m}{\hbar^3} \left| \lambda^3 \frac{dU}{dx} \right| << 1, \tag{39}$$

where x has the order of the barrier width. In our case, the left side of Eq. (39) has the values of the order of 10^{-4}, *i.e.*, less than unity.

5. RESULTS AND DISCUSSION

In the process of experiment for the determination of the contact angle of wetting of the steel substrate with liquid tin depending on temperature, we have found a decrease in the contact angle with the temperature rise. However, as the temperature rose further, the contact angle increased again [34]. Figure 3 shows photographs of a drop for three characteristic temperatures.

The results of experimental study of the formation of a contact angle and the work of adhesion depending on temperature for the system of tin–steel AISI 201 are given in Figs. 4 and 5. From these figures, it is clear that at first the values of the contact angle of this system decrease; the wetting threshold is observed at the temperature of $\cong 600$ K, and the dependence has a minimum at the temperature of 650 K. Values of the contact angle of wetting and the work of adhesion at 650 K are equal to 55° and 0.913 J/m^2. Further, with the rising temperature, the angle value increases and, at the temperature of 725 K, it is equal to 112°. Accordingly, the work of adhesion at this temperature is of 0.363 J/m^2. Therefore, we can determine the effect of abnormal

a *b* *c*

Fig. 3. Photograph of drop of liquid tin on substrates made of steel AISI 201 at the temperatures of 550 K (*a*), 650 K (*b*), and 775 K (*c*).

increase in the contact angle of wetting of the system tin–steel AISI 201, which is confirmed by experimental data.

For the comparison with the experimental results, Figures 4, 5 show the dependences of the contact angle of wetting and the work of adhesion on temperature, obtained by the given theoretical method for the tin–iron system. Mass of the tin atom was considered as m_1, and mass of the iron atom was taken as m_2. Calculations were carried out at $\tau = 12$ min, starting from the temperature of 525 K. At the given temperature, the energy $E - U$ of the system was equal to $3.57 \cdot 10^{-21}$ J, and the value of kinetic energy K was of $3.62 \cdot 10^{-21}$ J, comparable to $E - U$, with the quantum number $n = 6$. The calculations show that the energy required for changing of the quantum number from 6 to 6.5 is of $0.62 \cdot 10^{-21}$ J, while the energy required for transition of the system to the new level is of $1.29 \cdot 10^{-21}$ J. Consequently, values of the corresponding temperatures are of 614 K and 711 K. Values of the work of adhesion were calculated up to 614 K under Eqs. (29) and (33), in the temperature range of 614–711 K, according to Eqs. (29) and (37). When the temperature increased further above 711 K, the expression (33) was used again to calculate U.

Values of the contact angle and work of adhesion at the temperature of 525 K were of 122° and 0.272 J/m^2, respectively (Figs. 4, 5). At the temperature of 614 K, the quantum number changed from the integer to half-integer and values of these characteristics were of 60° and 0.868 J/m^2. As the temperature rose further, values of the contact angle decreased and those of the work of adhesion increased. The minimum dependence of the contact angle values on the temperature was observed at $T = 700$ K being equal to 28°. Accordingly, the value of the work of adhesion at this temperature was of 1.092 J/m^2. With the further increase in temperature, the system transitioned to the next energy level, and the wetting deteriorated. Therefore, at the temperature

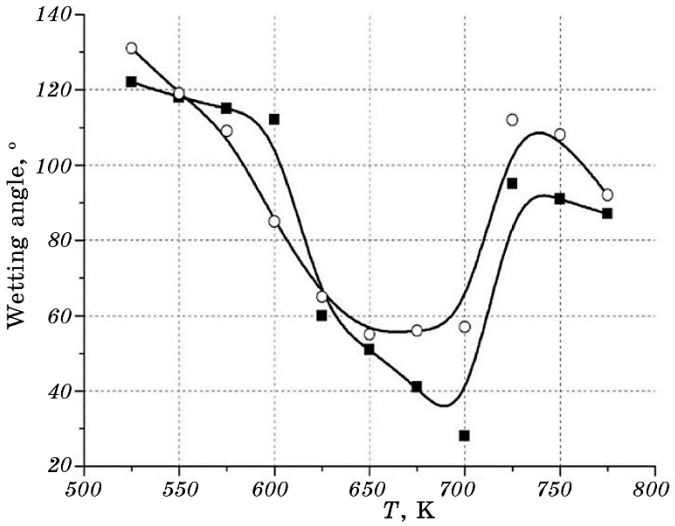

Fig. 4. Temperature dependence of the wetting angle: curve constructed experimentally (○), curve constructed by calculation (■).

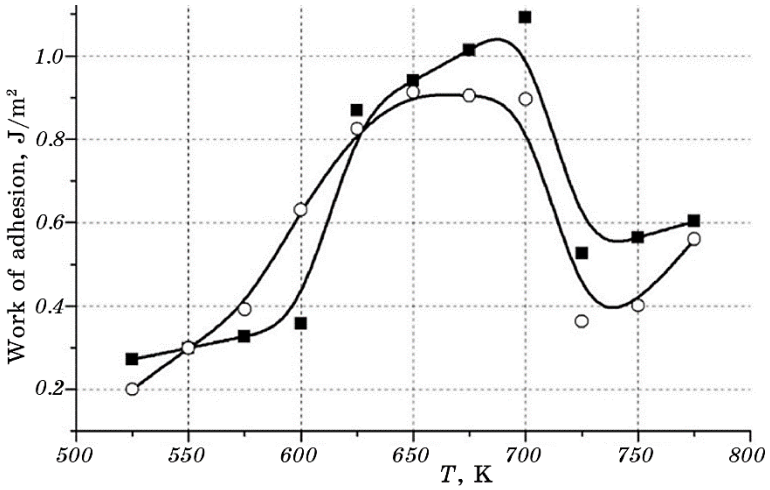

Fig. 5. Temperature dependence of adhesion: curve constructed experimentally (○), curve constructed by calculation (■).

of 725 K, the values of the contact angle and work of adhesion were of 95° and 0.526 J/m², respectively. Then, the contact angle values decreased.

The convergence of experimental data with the calculated ones shows that the proposed model used to calculate the work of adhesion and contact angle of non-equilibrium systems describes the observed

phenomena well.

The authors of Refs. [23, 24, 35, 36] suggest that the phenomenon of a sharp decrease in the contact angle of wetting at the temperature rise, *i.e.*, the wetting threshold, arises owing to the destruction of oxide films or the occurrence of chemical compounds between the solid and liquid phases. However, in our study no iron atoms were detected on the surface of the tin drop during the investigation by the x-ray fluorescence and atomic absorption methods after the experiment. Insignificant amount of nitrogen oxides was found on the surface of the tin drop by the ion-selective method. Nevertheless, it could not significantly affect the contact-angle dependence on the temperature. Since the proposed theoretical method for the calculation of the contact angle does not take into account the factors of nitrogen oxide formation, some discrepancies are observed in the constructed theoretical and experimental curves of dependence of the contact angle and adhesion on temperature.

Insignificant shift can also be explained by the fact of use of multicomponent steel substrate in the experiment, while pure iron was used in the calculations. Consideration of multicomponent systems will be the subject of our further studies. According to this model, the wetting threshold phenomenon arises owing to the fact that the system thermal energy exceeds the required value and the condition of a particle reflection from the potential barrier is satisfied. The other factor is the change in the ratio of linear dimensions of the barrier and the de Broglie wavelength from integer to half-integer. Therefore, the method proposed in this paper explains the observed phenomena during the contact of the liquid and solid phases in a different way, relying on quantum effects of the systems.

Previous studies in the systems of tin–steel and tin–iron [23, 24] did not reveal any abnormal increase in the contact angle depending on the temperature, since, for a heated system in equilibrium, the temperature rise cannot cause an increase in the contact angle of wetting [37]. Therefore, if a drop of tin is continuously heated to the certain temperature, the contact angle shall decrease, and it does not increase any longer with the rise in temperature. In our study, for each point of temperature dependence of the contact angle, a new drop of tin was examined each time with a step of 25 K. In this regard, at the temperature of about 725 K, as a result of changes in the interaction processes of the system, the contact angle initially did not reach small values that were observed at lower temperatures. The increase in wetting angle in the tin–steel system is observed, according to our ideas, as a result of changing energy of interaction between the melt and substrate atoms, as described by our model based on the WKB quasi-classical quantum conception.

This method can be used for the metallic non-equilibrium systems,

and we consider promising to study its application for non-metallic systems. The use of this method will allow predicting the processes in non-equilibrium systems by calculations, without conducting any experiments; so, it can find practical use in the creation of composite materials, soldering processes and solving of other applied problems.

6. CONCLUSION

We carried out the experimental observation of wetting of the solid substrate of steel AISI 201 with liquid tin. The temperature was increased in steps of 25 K, and for each fixed point of dependence, a new drop of tin was supplied on the substrate and examined. The wetting threshold is observed at $\cong 600$ K on the experimental curve of temperature dependence of the contact angle of wetting of this system. Therefore, decrease in the angle and increase in the work of adhesion corresponds to improved wetting. Further, with the temperature rise, the contact angle begins to increase abnormally and the work of adhesion decreases.

The abnormal effect of the sharp change in the wetting angle depending on temperature at the contact of the solid and liquid phases is described using the quasi-classical approximation of quantum mechanics. According to our ideas, the sharp change in the contact angle is explained by changing ratio of linear dimensions of the barrier and the de Broglie wavelength of the system.

The wetting threshold temperature is defined as the temperature, at which the condition of reflection of a particle with the reduced mass from the potential barrier determined by interaction energy of the contacting phases is satisfied.

The experimental curve of change in the contact angle of the system of tin–steel AISI 201 agrees satisfactorily with the theoretical curve for the tin–iron system. Thus, the proposed method of calculation can be used to find wetting indicators in non-equilibrium melt–solid metal systems.

This work was performed within the research ‘Adhesion Strength of the Galvanic Coatings’ (No. 0121U13278 of the State registration), ‘Development of Plasma Technologies for Strengthening Coatings Used in Extreme Conditions’ (No. 0123U104531 of the State registration).

REFERENCES

1. M. Malaki, A. F. Tehrani, B. Niroumand, and M. Gupta, *Metals*, **11**, No. 7: 1034 (2021).
2. D. Kumar Rajak, D. D. Pagar, R. Kumar, and C. I. Pruncu, *J. Mater. Res. Technol.*, **8**, No. 6: 6354 (2019).

3. D. Kumar Rajak, D. D. Pagar, P. L. Menezes, and E. Linul, *Polymers*, **11**, No. 10: 1667 (2019).
4. O. V. Sukhova and Yu. V. Syrovatko, *Metallofiz. Noveishie Tekhnol.*, **41**, No. 9: 1171 (2019) (in Russian).
5. O. V. Sukhova and Yu. V. Syrovatko, *J. Phys. Electronics*, **26**, No. 2: 29 (2018).
6. J. Avenet, A. Levy, J.-L. Bailleul, S. L. Corre, and J. Delmas, *Composites A: Appl. Sci. Manufact.*, **138**: 106054 (2020).
7. F. Delannay, L. Froyen, and A. Deruyttere, *J. Mater. Sci.*, **22**: 1 (1987).
8. Y. Wang, C. J. Hansen, C.-C. Wu, E. J. Robinettec, and A. M. Peterson, *RSC Adv.*, **11**: 31142 (2021).
9. C. Bistafa, D. Surblys, H. Kusudo, and Ya. Yamaguchi, *J. Chem. Phys.*, **155**, No. 6: 064703 (2021).
10. R. A. Kutuev, *Adv. Eng. Res.*, **177**: 152 (2018).
11. P. Fiflis, A. Press, W. Xu, D. Andruczyk, D. Curreli, and D. N. Ruzic, *Fusion Eng. Des.*, **89**: 2827 (2014).
12. D. A. Kambolov, A. Z. Kashezhev, R. A. Kutuev, P. K. Korotkov, A. R. Manukyants, M. Kh. Ponezhev, and V. A. Sozaev, *J. Surf. Investigation. X-ray, Synchrotron and Neutron Techniques*, **9**: 636 (2015).
13. N. V. Dalakova, K. M. Elekoeva, A. Z. Kashezhev, A. R. Manukyants, A. D. Prokhorenko, M. Kh. Ponezhev, and V. A. Sozaev, *J. Surf. Investigation. X-ray, Synchrotron and Neutron Techniques*, **8**: 360 (2014).
14. M. Kondo and J. Matsumoto, *Computer Methods Appl. Mech. Eng.*, **385**: 114072 (2021).
15. M. Provenzano, F. M. Bellussi, M. Morciano, E. Rossi, M. Schleyer, P. Asinari, T. Straub, M. Sebastiani, and M. Fasano, *Mater. Des.*, **231**: 112042 (2023).
16. N. Mukai, T. Natsume, M. Oishi, and M. Oshima, *Proc. 18th Int. Joint Conf. on Computer Vision, Imaging and Computer Graphics Theory and Applications (Feb. 19–21, 2023)* (Lisbon: VISIGRAPP: 2023), vol. **1**, p. 230.
17. J.-Y. Lu, C.-Y. Lai, I. Almansoori, and M. Chiesa, *Phys. Chem. Chem. Phys.*, **20**: 22636 (2018).
18. J. Y. Lu, Q. Ge, H. Li, A. Raza, and T. J. Zhang, *J. Phys. Chem. Lett.*, **8**, No. 21: 5309 (2017).
19. J. Y. Lu, Q. Ge, A. Raza, and T. J. Zhang, *J. Phys. Chem. C*, **123**, No. 20: 12753 (2019).
20. H. Peng, A. V. Nguyen, and G. R. Birkett, *Molecular Simulation*, **38**, No. 12: 945 (2012).
21. B. Zhang, H. Li, Z. W. Zhu, H. M. Fu, A. M. Wang, C. Dong, H. F. Zhang, and Z. Q. Hu, *Mater. Sci. Technol.*, **29**, No. 3: 332 (2013).
22. S. Mettu, M. Kanungo, and K. Law, *Langmuir*, **29**, No. 34: 10665 (2013).
23. D. Varanasi, K. E. Aldawoudi, P. Baumli, D. Koncz-Horvath, and G. Kaptay, *Arch. Metall. Mater.*, **66**, No. 2: 469 (2021).
24. S. I. Popel, V. N. Kozhurkov, and T. V. Zakharova, *Zashchita Metallov*, **7**, No. 4: 421 (1971) (in Russian).
25. G. V. Beketov and O. V. Shynkarenko, *Him. Fiz. Tehnol. Poverhni*, **13**, No. 1: 3 (2022).
26. V. T. Shipatov and P. P. Seregin, *Theoretical Exp. Chem.*, **8**: 343 (1974).
27. O. V. Sukhova and Yu. V. Syrovatko, *Visnyk ZhDTU*, **82**, No. 2:189 (2018) (in Ukrainian).
28. D. E. Packham, *Int. J. Adhes. Adhes.*, **16**, No. 2: 121 (1996).

29. F. Hejda, P. Solar, and J. Kousal, *Proc. 19th Annual Conf. Doctoral Students (June 1–4, 2010)* (Prague: WDS: 2010), vol. **3**, p. 25.
30. ДСТУ 7538:2014. *Vyznachennya Nitrativ Ionometrychnym Metodom* [Determination of Nitrates by the Ionometric Method] (Kyiv: Minekonomrozvytku of Ukraine: 2015) (in Ukrainian).
31. ДСТУ 4770.1:2007. *Vyznachennya Vmistu Rukhomykh Spoluk Zaliza v Kyslotniy Vytyazhtsi Metodom Atomno-Adsorbtsiynoyi Spektrofotometriyi* [Determination of the Content of Mobile Iron Compounds in the Acid Extract by the Method of Atomic Adsorption Spectrophotometry] (Kyiv: Derzhspozhyvstandart of Ukraine: 2007) (in Ukrainian).
32. ДСТУ 8899:2019. *Stal'. Metod Rentgenofluorestsentnoho Analizu* [Steel. X-Ray Fluorescence Analysis Method] (Kyiv: UkrNDNTs: 2021) (in Ukrainian).
33. L. D. Landau and L. M. Lifshitz, *Quantum Mechanics: Non-Relativistic Theory* (Oxford: Pergamon Press: 1977).
34. E. Ph. Shtapenko and Yu. V. Syrovatko, *Proc. All-Ukrainian Scientific and Technical Conf. 'Science and Metallurgy' (November 14–16, 2023)* (Dnipro: Iron and Steel Institute N.A.S. of Ukrainian: 2023), p. 51 (in Ukrainian).
35. D. A. Kambolov, A. Z. Kashezhev, R. A. Kutuev, A. R. Manukyants, M. Kh. Ponegev, V. A. Sozaev, and A. Kh. Shermetov. *J. Surf. Investigation. X-ray, Synchrotron and Neutron Techniques*, **10**: 1276 (2016).
36. B. B. Alchagirov and K. B. Khokonov, *High Temp.*, **32**, No. 4: 553 (1994).
37. F. Villa, M. Marengo, and J. D. Coninck, *Sci. Rep.*, **8**: 6549 (2018).